



Deposited via The University of Sheffield.

White Rose Research Online URL for this paper:

<https://eprints.whiterose.ac.uk/id/eprint/145422/>

Version: Accepted Version

---

**Article:**

Bernut, A., Le Moigne, V., Lesne, T. et al. (2014) In vivo assessment of drug efficacy against *Mycobacterium abscessus* using the embryonic zebrafish test system.

*Antimicrobial Agents and Chemotherapy*, 58 (7). pp. 4054-4063. ISSN: 0066-4804

<https://doi.org/10.1128/aac.00142-14>

---

© 2014 American Society for Microbiology. This is an author-produced version of a paper accepted for publication in *Antimicrobial Agents and Chemotherapy*. Uploaded in accordance with the publisher's self-archiving policy.

**Reuse**

Items deposited in White Rose Research Online are protected by copyright, with all rights reserved unless indicated otherwise. They may be downloaded and/or printed for private study, or other acts as permitted by national copyright laws. The publisher or other rights holders may allow further reproduction and re-use of the full text version. This is indicated by the licence information on the White Rose Research Online record for the item.

**Takedown**

If you consider content in White Rose Research Online to be in breach of UK law, please notify us by emailing [eprints@whiterose.ac.uk](mailto:eprints@whiterose.ac.uk) including the URL of the record and the reason for the withdrawal request.

1                    ***In vivo* assessment of drug efficacy against *Mycobacterium***  
2                    ***abscessus* using the embryonic zebrafish test system**

3  
4                    **Audrey Bernut<sup>1</sup>, Vincent Le Moigne<sup>3</sup>, Tiffany Lesne<sup>1</sup>, Georges Lutfalla<sup>1</sup>,**  
5                    **Jean-Louis Herrmann<sup>3</sup> and Laurent Kremer<sup>1,2,#</sup>**  
6  
7

8                    <sup>1</sup>Laboratoire de Dynamique des Interactions Membranaires Normales et Pathologiques,  
9                    CNRS UMR5235, Université Montpellier 2, Montpellier, France ;

10                    <sup>2</sup>Inserm, DIMNP, Place Eugène Bataillon, 34095 Montpellier Cedex 05, France.

11                    <sup>3</sup>EA3647-EPIM, UFR des Sciences de La Santé; Université de Versailles St Quentin, 2 avenue  
12                    de la Source de la Bièvre, 78180 Montigny le Bretonneux, France.

13

14

15                    #To whom correspondence should be addressed:

16                    Tel: (+33) 4 67 14 33 81, Fax: (+33) 4 67 14 42 86, E-mail: [laurent.kremer@univ-montp2.fr](mailto:laurent.kremer@univ-montp2.fr)

17

18                    **Keywords:** *M. abscessus*, zebrafish, drug testing, optical imaging, infection

19

20                    **Running title:** *In vivo* imaging for anti-*M. abscessus* drug testing

21

22

23 **ABSTRACT**

24

25 *Mycobacterium abscessus* is responsible for a wide spectrum of clinical syndromes and is  
26 one of the most intrinsically drug-resistant mycobacterial species. Recent evaluation of the  
27 *in vivo* therapeutic efficacy of the few potentially active antibiotics against *M. abscessus* was  
28 essentially performed using immune-compromised mice. Herein, we assessed the feasibility  
29 and sensitivity of fluorescence imaging for monitoring the *in vivo* activity of drugs against  
30 acute *M. abscessus* infection using zebrafish embryos. A protocol was developed where  
31 clarithromycin and imipenem were directly added to water containing fluorescent *M.*  
32 *abscessus*-infected embryos in a 96-well plate format. The status of the infection with  
33 increasing drug concentrations was visualized on a spatiotemporal level. Drug efficacy was  
34 assessed quantitatively by measuring the index of protection, the bacterial burden (CFU) and  
35 the number of abscesses through fluorescence measurements. Both drugs were active in  
36 infected embryos and were capable of significantly increasing embryo survival in a dose-  
37 dependent manner. Protection from bacterial killing correlated with restricted mycobacterial  
38 growth in the drug-treated larvae and with reduced pathophysiological symptoms, such as  
39 the number of abscesses within the brain. In conclusion, we present here a new and efficient  
40 method for testing and compare the *in vivo* activity of two clinically-relevant drugs based on  
41 a fluorescent reporter strain in zebrafish embryos. This approach could be used for rapid  
42 determination of *in vivo* drug susceptibility profile of clinical isolates and to assess the  
43 preclinical efficacy of new compounds against *M. abscessus*.

44

45 **INTRODUCTION**

46

47 The emerging pathogen *M. abscessus* (*Mabs*) is the etiological agent of a wide spectrum  
48 of infections in humans including severe chronic pulmonary and disseminated infections,  
49 mostly in immunosuppressed and in cystic fibrosis (CF) patients (1), and cutaneous diseases,  
50 often post-traumatic and post-surgical. This neglected pathogen causes a higher fatality rate  
51 than other Rapidly Growing Mycobacteria (RGM) and CF patients infections is becoming a  
52 major threat in most CF centers worldwide (2). *Mabs* infections occur in early childhood (3),  
53 are severe and sometimes fatal, especially following transplantation (4-6), and may lead to  
54 outbreaks of infection (6). It is also the main RGM responsible for nosocomial and iatrogenic  
55 infections in humans (post-injection abscesses, cardiac surgery, and plastic surgery) (7-9). It  
56 has been reported to cross the blood-brain barrier and cause important central nervous  
57 system (CNS) lesions. Although rapid grower, *Mabs* possesses several important pathogenic  
58 traits such as the ability to i) persist silently for years and even decades (10) in the human  
59 host, and to ii) induce lung disease with caseous lesions and granuloma formation in the  
60 parenchyma (11, 12).

61 The major issue with *Mabs* relies on its intrinsic resistance to the most available  
62 antibiotics. The American Thoracic Society has recommended different groups of agents,  
63 namely macrolides (clarithromycin), aminoglycosides (amikacin), cephamycins (cefoxitin)  
64 and carbapenems (imipenem) to treat *Mabs* infections (13). Patients with severe infections  
65 are generally treated with long courses of combinatorial antibiotic therapy, often backed by  
66 surgical resection. As antibiotic susceptibility testing is not fully standardized, the clinical  
67 response to drugs does not correlate well with *in vitro* susceptibility tests and failure occurs  
68 frequently despite administration of two or three antibiotics for several months (14). This

69 further emphasizes the need for suitable animal models (15, 16). In addition, different  
70 clinical isolates of this emerging pathogen are not uniformly susceptible to currently used  
71 antibiotics (17). As a consequence, an optimal regimen to cure the *Mabs* infections has not  
72 been yet established.

73 Thanks to the recent availability of efficient genetic tools (18), *Mabs* has been proposed  
74 as an attractive experimental model to study non-tuberculous mycobacteria associated  
75 diseases. Our poor understanding of the pathogenesis of *Mabs*, essentially hampered by the  
76 restricted panel of cellular/animal models available, prompted us to develop the zebrafish  
77 (ZF) model of infection evaluate *Mabs* infections (19). In particular, the *Mabs*/zebrafish  
78 model already provided important insights into *Mabs* pathogenesis including the unexpected  
79 CNS tropism, a finding relevant in the light of recent clinical studies reporting the presence  
80 of *Mabs* in the CNS of infected human patients (20, 21). Since infection foci/abscesses within  
81 the CNS, particularly the brain, appear very rapidly and are easily visualized, we reasoned  
82 that this alternative model could represent a valuable and cheap system to evaluate and  
83 compare the *in vitro* and *in vivo* activity of drugs against *Mabs*. Such a simple and innovative  
84 system would be particularly suited to screen active molecules and/or assess antibacterial  
85 activities for the discovery of the urgently needed drugs to fight *Mabs*.

86 Here, we report experimental conditions for spatiotemporal *in vivo* imaging of *Mabs*  
87 infections and their use to test the efficacy of drug treatments. This represents a unique  
88 biological model allowing non-invasive observations to evaluate, in real time, the efficacy of  
89 antibiotics in living infected vertebrates, a system that could be applied to high-throughput  
90 *in vivo* testing of drug efficacy against the most drug-resistant mycobacterial species.

91

92 **MATERIALS AND METHODS**

93

94 ***M. abscessus* strains and growth conditions**

95 The rough variant of *M. abscessus sensu stricto* strain CIP104536<sup>T</sup> (ATCC19977T) (R-  
96 *Mabs*) was grown at 30°C in Middlebrook 7H9 broth supplemented with 10% Oleic  
97 acid/Albumin/Dextrose/Catalase (OADC) enrichment and 0.05% Tween 80 (7H9<sup>T</sup>) or on  
98 Middlebrook 7H10 agar containing 10% OADC (7H10). Recombinant *Mabs* carrying pTEC27  
99 (Addgene, plasmid 30182) that allows to express the tdTomato fluorescent protein under  
100 the control of a strong mycobacterial promoter were grown in the presence of hygromycin  
101 500 mg/L (19).

102

103 **Mice experiments and CFU counting**

104 6-8 weeks old BALB/c mice were divided in groups of 5-7 mice and used for either  
105 intravenous (*i.v.*) or aerosol challenges. Inocula were prepared from rapidly thawed frozen  
106 aliquots, and bacterial clumps were eliminated by iterative passages through a 29.5-gauge  
107 insulin needle (Becton Dickinson). Bacterial suspensions were then diluted in phosphate  
108 buffer saline (PBS). For *i.v.* inoculations, 10<sup>6</sup> CFU (in 200 µl) were injected into the lateral  
109 tail/caudal vein, as previously described (22, 23). Pulmonary infections were achieved with  
110 aerosolized *Mabs* using an aerosol generator, equipped with a Micro Mist<sup>®</sup> small volume  
111 nebulizer (Hudson RCI-Teleflex medical) containing 6 ml of bacterial solution at 4 × 10<sup>7</sup>  
112 CFU/ml. Pre-sleeping mice (isoflurane<sup>®</sup> Abbott) were anesthetized with 200 µl of  
113 Hypnomidate (Etomidate<sup>®</sup>, Janssen-Cilag) and placed into an opened 50 ml syringe fixed on  
114 the top of a closed compartment containing the nebulizer. In this device, nebulization lasted  
115 for 15 min to vaporize the entire bacterial suspension. Lungs, liver and spleen were collected

116 in PBS, crushed and 10-folds serial dilutions were plated on Middlebrook 7H11 plates for CFU  
117 counting, as previously described (22, 23). Plates were then incubated at 37°C for up to 7  
118 days. The results were expressed as the mean Log<sub>10</sub> CFU per organ.

119

#### 120 **Minimal inhibitory concentrations**

121 Antibiotics powder tested in drug susceptibility assays were pharmaceutical standards  
122 for imipenem/cilastatin (Mylan) or clarithromycin (Sigma-Aldrich). Stock solutions were  
123 dissolved in water (imipenem) or in DMSO (clarithromycin). Drug susceptibility testing was  
124 also determined using the microdilution method, in cation-adjusted Mueller-Hinton broth,  
125 according to the Clinical and Laboratory Standards Institute (CLSI) guidelines (24). In  
126 addition, the susceptibility profile was also determined on LB agar supplemented with  
127 increasing concentrations of compounds. Serial 10-fold dilutions of each actively growing  
128 culture were plated and incubated at 37°C for 3-4 days and the MIC was defined as the  
129 minimum concentration required to inhibiting 99% of the growth.

130

#### 131 **Zebrafish care and ethic statements**

132 All zebrafish experiments were done at the University Montpellier 2, according to  
133 European Union guidelines for handling of laboratory animals  
134 ([http://ec.europa.eu/environment/chemicals/lab\\_animals/home\\_en.htm](http://ec.europa.eu/environment/chemicals/lab_animals/home_en.htm)) and approved by  
135 the Direction Sanitaire et Vétérinaire de l'Hérault and Comité d'Ethique pour  
136 l'Expérimentation Animale de la région Languedoc Roussillon (CEEA-LR) under the reference  
137 CEEA-LR-13007. Experiments were done using the *golden* ZF mutant (25), maintained as  
138 described earlier (19). Ages of embryos are expressed as hours post fertilization (hpf).

139

140       **Microinjection of *M. abscessus* into embryos**

141       Mid-log phase cultures of *Mabs* expressing tdTomato were centrifuged, washed and  
142 resuspended in PBS supplemented with 0.05% Tween-80 (PBS<sup>T</sup>). Bacterial suspensions were  
143 then homogenized through a 26-gauge needle and sonicated and the remaining clumps were  
144 allowed to settle down to for 5-10 min, as previously described (19). Bacteria were  
145 concentrated to an OD<sub>600</sub> of 1 in PBS<sup>T</sup> and *i.v.* injected (≈2nL containing 300 CFU) into the  
146 caudal vein in 30hpf embryos previously dechorionated and anesthetized. To follow  
147 infection kinetics and embryo survival, infected larvae were transferred into 96 well plates (2  
148 embryos/plate) and incubated at 28.5°C. The inoculum size was checked by injection of 2nL  
149 in sterile PBS<sup>T</sup> and plated on 7H10 supplemented with hygromycin 500 mg/L.

150

151       **Drug efficacy assessment in *Mabs*-infected ZF**

152       Clarithromycin and imipenem/cilastatin were added at one day post-infection (dpi),  
153 directly into the water containing the embryos. Three doses were tested, corresponding to  
154 1.7X, 17X and 170X the MIC of clarithromycin and 0.5X, 5X or 28X the MIC of imipenem,  
155 based on the values determined using the microdilution method (Table S1). *In vivo* drug  
156 efficacy was determined for each concentration by following i) bacterial burdens, ii) kinetics  
157 of embryo survival, iii) evolution of the infection foci/abscesses within the CNS and iv) effect  
158 on bacterial cord formation/reduction. Survival curves were determined by recording dead  
159 embryos (no heartbeat) every day for up to 13 days. Regarding the kinetic of mycobacterial  
160 loads, groups of three infected embryos were collected, lysed individually in 2% Triton X100-  
161 PBS<sup>T</sup> with a 26-gauge needle and resuspended in PBS<sup>T</sup>. Several 10-fold dilutions of  
162 homogenates were plated on 7H10, the appropriate antibiotics and added of mix of “BBL<sup>TM</sup>

163 MGIT™ PANTA™ (Becton-Dickinson) using as recommended by the supplier. CFU were  
164 enumerated after 4 days of incubation at 30°C. This procedure was repeated at 0, 3, 5 dpi.

165

#### 166 **Microscopy**

167 Widefield bright-field and fluorescence live microscopy of infected embryos were  
168 performed using an Olympus MVX10 epifluorescent microscope equipped with a X-  
169 Cite® 120Q (Lumen Dynamics) 120W mercury light source. Images are acquired with a digital  
170 color camera (Olympus XC50) and processed using CellSens software (Olympus).  
171 Fluorescence filter cube TRITC-MVX10 is used for detection of red light. For live imaging,  
172 anesthetized infected embryos were positioned in dishes and immobilized with 1% low-  
173 melting point agarose solution covering the entire larvae then immobilized embryos are  
174 immersed with fish water containing tricaine for direct visualization.

175

#### 176 **Image Processing and Analysis**

177 Final images analysis and visualization are performed using GIMP 2.6 freeware to merge  
178 fluorescent and DIC images and to adjust levels and brightness and to remove out-of-focus  
179 background fluorescence.

180

#### 181 **Statistical Analyses**

182 Statistical analyses of comparisons between Kaplan-Meier survival curves were  
183 performed using the log rank test with Prism 4.0 (Graphpad, Inc). CFU counts and  
184 quantifications experiments were analyzed using one-way ANOVA and Fisher's exact test,  
185 respectively. Statistical significance was assumed at  $p$  values <0.05.

186

187 **RESULTS**188 ***M. abscessus* fails to establish a persistent infection in BALB/c mice**

189 Experiments were first aimed at determining the colonization rate of R-*Mabs* in a murine  
190 pulmonary infection model (Figure 1A). Aerosol infections of BALB/c mice led to an initial and  
191 rapid increase of the bacterial burden from 1-3 days post-infection (dpi) in the lungs, followed  
192 by a phase of infection control leading to a reduction (starting after 3dpi) and almost  
193 complete clearance of the bacilli at 27dpi. Very few bacteria were detected within the spleen  
194 or the liver of infected mice. The colonization profile after *i.v.* challenge showed that bacilli  
195 were primarily found in the liver at 1dpi and to a lesser extent in the spleen and lungs (Figure  
196 1B). All heavily infected organs rapidly underwent a progressive reduction in bacterial loads  
197 with a 3-Log<sub>10</sub> CFU decrease in the liver and lungs at 30dpi, highlighting a transient  
198 colonization process. This indicates that immune-competent mice steadily eradicate the  
199 pathogen and therefore that wild-type BALB/c mice are not well adapted to investigate the *in*  
200 *vivo* efficacy of therapeutic treatments. This would require testing a very large number of  
201 animals to insure that the observed CFU decrease results from an antibiotic regimen rather  
202 than from the natural course of infection. This highlights the need of an alternative animal  
203 model, susceptible to *Mabs* infection, permissive to bacterial replication and leading to the  
204 development of infection foci/abscesses and death. Therefore, the ZF embryo model was  
205 chosen to test *in vivo* assessments of drugs against *Mabs*.

206

207 **Zebrafish larvae for *in vivo* assessment of drug activity in *M. abscessus***

208 An experimental protocol was designed to assess *in vivo* antimycobacterial drug activity  
209 against *Mabs* in ZF larvae (Figure 2). Red fluorescent tdTomato-expressing R-*Mabs* were  
210 injected in the caudal vein of embryos at 30 hours post-fertilization (hpf) and transferred

211 into 96-well plates. Antibiotics were directly added at 1dpi to the water containing the  
212 infected embryos and the drug-supplemented water was then changed on a daily basis for 5  
213 days. Thanks to the optical transparency of the embryos, daily microscopic recording of  
214 mortality (transmission) as well as bacterial burden (fluorescence) were used as phenotypic  
215 read-outs. We have previously shown that the rough *Mabs* exhibits a marked neurotropism  
216 with massive abscesses within the CNS (19), thus prompting us to assess the  
217 chemotherapeutic activity of drugs in *Mabs*-infected embryos with a special emphasis on  
218 infection within the CNS (Figure 2). Drug-mediated toxicity was investigated by checking  
219 survival curves of non-infected embryos treated with increasing drug doses.

220

#### 221 **Minimal inhibitory concentrations of antimycobacterial drugs against *M. abscessus***

222 We first determined the *in vitro* activity of various drugs, including antitubercular  
223 agents, against *Mabs* using microdilution in cation-adjusted Mueller-Hinton broth, according  
224 to the Clinical and Laboratory Standards Institute guidelines (24). Table S1 shows that the  
225 activity varies considerably, in agreement with other studies (17). The first-line  
226 antitubercular drug isoniazid and second-line drug thiacetazone appeared inactive against  
227 *Mabs*. Among the few clinically used drugs for the treatment of *Mabs* infection, cefoxitin,  
228 amikacin, imipenem and erythromycin exhibit moderate activity *in vitro* on agar plates with  
229 MICs ranging from 60-125  $\mu$ M, whereas clarithromycin demonstrated the highest activity  
230 with an MIC value of 4  $\mu$ M. Because clarithromycin and imipenem exhibit different  
231 physicochemical properties (high molecular weight and hydrophobicity for clarithromycin  
232 versus low molecular weight and hydrophilicity for imipenem), they were further  
233 investigated for their *in vivo* therapeutic efficacy in *Mabs*-infected ZF.

234

235 ***In vivo* susceptibility of *M. abscessus* to clarithromycin**

236 Due to poor information concerning the mechanisms of drug uptake by ZF  
237 embryos/larvae, we tested a wide range of clarithromycin concentrations: 6.6  $\mu\text{M}$  to 668  $\mu\text{M}$   
238 (1.7X to 170X the *in vitro* MIC value from the microdilution method). Supplementing the  
239 embryo-containing water with low or intermediate doses (1.7X and 17X the MIC,  
240 respectively) led to no toxicity as measured by larval survival, while the highest tested dose  
241 (170X MIC), led to a 10% reduction in larval survival at 9dpi, with respect to the control  
242 group (water with 1% DMSO; Figure 3A) (26). In the presence of high doses of  
243 clarithromycin, embryos had a curved body trunk with un-inflated swim bladder (Figure 3A,  
244 inset). These phenotypic alterations were hardly observed when exposed to intermediate or  
245 low doses of clarithromycin (not shown).

246 No significant increased survival was found when infected-embryos were exposed to  
247 low and intermediate drug concentrations (Figure 3B). In contrast, high doses extended the  
248 life span of infected embryos and fully protected the infected embryos up to 9dpi, when the  
249 first embryo started to dye, which coincidentally, corresponded to the toxicity-induced-killing  
250 effect (Figure 3A). This shows that clarithromycin, using the highest regimen, is efficient in  
251 the ZF test system.

252

253 **Effects of clarithromycin on ZF survival, bacterial burden and abscesses**

254 Increased survival was associated with lower bacterial burdens after 3dpi in the  
255 presence of the highest dose (170X MIC), as determined quantitatively by CFU plating  
256 (Figure 3C), whereas treatment with the low or intermediate doses failed to restrict  
257 mycobacterial growth. *In vivo* drug efficacy was next monitored by time-lapse fluorescence  
258 microscopy (Figure 3D) of the rapidly growing infection foci and abscesses in the larval brain

259 (19). Imaging the same infected embryos at 3 and 5dpi revealed that abscesses within the  
260 brain were already reduced at 3dpi when treated with high drug concentrations and this  
261 reduction of the clinical signs of infection was even more accentuated at 5dpi. Consistent  
262 with the survival curves and kinetic of bacterial growth, there was no visible reduction of the  
263 infection at 5dpi in ZF treated with low or intermediate drug concentrations. Quantitative  
264 analysis reveals that high doses of clarithromycin reduced by 50% the number of embryos  
265 with abscesses (Figure 3E) both in the brain and the spinal cord (Figure 3F). This indicates  
266 that clarithromycin exerts a therapeutic effect by inhibiting mycobacterial growth,  
267 preventing the development of abscesses within the CNS and protecting the embryos from  
268 bacterial killing.

269

#### 270 **Effects of imipenem on ZF survival and reduction of the pathological signs**

271 Imipenem is a clinically relevant drug against *Mabs* known to act on L, D-transpeptidases  
272 (17, 27). Concentrations from 0.5X to 28X MIC of imipenem were tested, which all fail to  
273 display signs of toxicity-induced-killing or developmental abnormalities (data not shown).  
274 When assessing the effect of imipenem on infected ZF, no increased survival was found with  
275 low drug concentrations. However, treatment with intermediate doses led to a significant  
276 increase in survival and 100% of protection was observed in the presence of the highest drug  
277 concentration (Figure 4A). These survival rates correlated with CFU loads as intermediate  
278 and high doses of imipenem started to restrict bacterial growth at 3dpi (after two days of  
279 drug treatment) (Figure 4B). With the highest dose, there was a 3 Log<sub>10</sub> decrease in CFU at  
280 5dpi (four days of treatment) compared with the untreated control group. Time-lapse  
281 fluorescence microscopy further confirmed the *in vivo* efficacy of imipenem at intermediate  
282 and high doses, illustrating the inhibition of bacterial growth and disappearance of abscesses

283 in the larval brain at 3 and 5dpi, respectively (Figure 4C). High doses significantly reduced the  
284 proportion of embryos with abscesses (Figure 4D), a phenotypic effect that was particularly  
285 apparent in the brain on infected embryos (Figure 4E), indicating that imipenem reduces the  
286 pathology signs of the infection.

287 These results prompted us to check whether imipenem can counteract/alter the  
288 progression of an already established infection, if given at 3dpi when brain abscesses are  
289 already apparent (Figure S1A). Death curves indicate that treatment with high doses of  
290 imipenem efficiently extended the life span of embryos with pre-existing abscesses (Figure  
291 S1B). A large proportion (more than 60%) of the treated embryos survived to the infection  
292 compared to 10% for the non-treated individuals ( $p=0.008$ ). The 40% embryos that died  
293 despite treatment showed increased bacterial loads in the CNS (data not shown). The  
294 increased index of protection rate was associated to a significant decrease in the number of  
295 embryos with abscesses (Figure S1C), particularly within the brain (Figure S1D). This  
296 “curative” protocol shows that imipenem was able to cure embryos with pre-existing  
297 abscesses and protect severely infected ZF.

298

#### 299 ***In vivo* inhibition activity of imipenem on mycobacterial cording**

300 Rough *Mabs* displays a dry texture with organized serpentine cords on agar plates (19,  
301 28, 29) and large bacterial clumps consisting mainly of cords in liquid cultures (19). Our  
302 recent studies also unraveled the presence of serpentine cords within the brain or spinal  
303 cord of embryos infected with the rough morphotype and emphasized the role of cording in  
304 immune evasion by preventing phagocytosis of *Mabs* by macrophages and neutrophils (19).  
305 Cords are easily visualized and counted by fluorescence microscopy (Figure 5A), and they  
306 promote extracellular replication, abscess formation and tissue damage (19). We checked

307 whether exposure of infected embryos to imipenem may affect the development of  
308 mycobacterial cords. Figure 5B shows the impact of imipenem treatment on the number of  
309 cords; quantitative analysis is shown in Figure 5C. The presence of low doses of imipenem  
310 has little impact on mycobacterial cords, although a reduction of the number of embryos  
311 with cords was detected at 4dpi. However, this effect was more pronounced with higher  
312 drug concentrations with only 20% of cord-laden embryos at 4dpi (compared to 60% for  
313 untreated embryos at 4dpi). This dose-dependent effect occurred essentially within the CNS  
314 whilst reduction of cord formation within the vasculature was not significant (Figure 5D).  
315

316 **DISCUSSION**

317       At a basic research level, the appropriate use of animal models can help to improve our  
318 understanding of host-pathogen interactions. At a more applied level, preclinical evaluation  
319 of new drugs requires *in vivo* testing prior to progressing along the development pipeline.  
320 However, *in vivo* animal studies, when possible, are usually costly and time-consuming and  
321 present a major bottleneck in drug developments. Implementation of novel approaches,  
322 expected to accelerate the *in vivo* assessment of drugs, is particularly justified in two cases.  
323 First, such systems are useful for bacterial infections requiring extended periods of drug  
324 treatment such as mice infected with *M. tuberculosis*, for which rapid *in vivo* assessment of  
325 drug efficacy directly in infected mice using fluorescence imaging (30) or using improved  
326 firefly luciferase (31) were elegantly demonstrated. We similarly show in this study how the  
327 use of fluorescence imaging can be useful in evaluating antimicrobial activity against *Mabs*.  
328 Second, alternative biological systems are particularly relevant for infections lacking of a  
329 permissive animal model. In this context, we recently demonstrated the high susceptibility of  
330 ZF embryos to *Mabs* (19) and how the number of CNS abscesses may represent a marker for  
331 establishing *in vivo* antibiotic activity against *Mabs*.

332       One of the key steps of drug discovery process is to identify and evaluate the *in vitro* and  
333 *in vivo* potential of new hits against *Mabs* using adapted animal models. The murine model  
334 in immune-competent BALB/c mice (*i.v.* or aerosol infections), led only to transient  
335 colonization, impeding its use as a valuable animal model for drug testing. Comparatively,  
336 SCID mouse model has been shown to produce a chronic infection of *Mabs*, but this model  
337 has not been used for drug testing (29, 32). Granulocyte-macrophage colony-stimulating  
338 (GM-CSF) knockout mice have recently been used to develop a new animal model of  
339 persistent pulmonary *Mabs* infection that can be used for preclinical efficacy testing of anti-

340 microbial drugs (15). Azithromycin treatment of *Mabs*-infected GM-CSF KO mice resulted in  
341 a lower bacterial burden in the lungs and spleen, weight gain and significant improvement in  
342 lung pathology (15). Another report proposed Nude mice as an adequate model for *in vivo*  
343 chemotherapy studies (16). However, both models raised the question of the adaptive  
344 response in addition to the antibiotic activity in eradicating the bacilli. It was previously  
345 shown that, albeit being a rapid-growing mycobacterium, *Mabs* infection was only controlled  
346 in mice with a functional adaptive immune response (22), as compared to *M. chelonae*,  
347 which was cleared even in T cell-deficient mice. Despite the fact that both immune-  
348 compromised mice present a significant advance as compared to wild-type mice in  
349 preclinical assessments, these models remain costly, time-consuming and, most likely, not  
350 suitable for a general use in drug screening strategies.

351 New non-mammalian models of infection have been developed, including *Drosophila*  
352 *melanogaster* (33, 34), *Caenorhabditis elegans* (35) or *Danio rerio* (36, 37) offering  
353 advantages in terms of speed, cost, technical convenience and ethical acceptability over the  
354 mouse model. Except for the recent *Drosophila* model (34), these models have not been  
355 reported for antibiotic assessments against *Mabs*. We propose here the ZF model to  
356 visualize, by non-invasive imaging, the progressive infection of *Mabs* in live animals, and to  
357 quantifying the effect of drug treatment. We successfully investigated the suitability and  
358 sensitivity of two clinically relevant drugs, clarithromycin and imipenem, to visualize in a  
359 dose- and time-dependent manner the dynamics of cord and abscess formation/resorption.  
360 One major advantage of this model, compared to mice, is the ease and rapidity of  
361 experimentation within a restricted time scale and low cost. That both drugs had a positive  
362 impact in terms of embryo survival was correlated to a significant reduction in the number of  
363 CFU and abscesses, demonstrating a proof of concept that ZF embryos are suitable for drug

364 efficacy testing. Since *in vitro* studies demonstrated decreased MICs in the presence of  
365 imipenem, for clarithromycin, minocycline, levofloxacin and moxifloxacin (38), future work  
366 should also address the *in vivo* efficacy of these drug combinations using the *Mabs*/ZF  
367 couple.

368 It is, however, noteworthy that despite their unique features for *in vivo* drug testing, ZF  
369 embryos also present several disadvantages over mammalian models. In particular, there are  
370 some important anatomical differences between ZF embryos and mammals such as gills  
371 instead of lungs, hematopoiesis occurring in the anterior kidney instead of the bone marrow,  
372 lack of discernable lymph nodes as well as a very different reproductive system. The natural  
373 lack of adaptive immunity early in the development is very likely to affect the outcome of  
374 the infection, thus making it difficult to directly correlating data obtained in ZF and in  
375 humans. In addition, as shown in this study, embryos are adapted to testing antibiotics  
376 during acute R-*Mabs* infections but not during the chronic stages of the disease, which can  
377 be better modelled for instance using immuno-compromized mice (15). Since  
378 pharmacokinetics are not known in ZF, it remains difficult at this stage to directly transpose  
379 the MIC data obtained in ZF to humans. As a consequence, this biological system should  
380 essentially be regarded as an early model for pre-clinical drug testing and/or to select new  
381 active compounds which should then be evaluated in other models before clinical trials.

382 The perspectives of application of the present findings are multiple. First, this method  
383 could be implemented to address the *in vivo* drug susceptibility profiles of clinical isolates  
384 including strains from CF and non-CF patients, as *Mabs* clinical strains are not uniformly  
385 susceptible to currently used antibiotics. Due to these strain-to-strain variations (17, 39), no  
386 optimal regimen has been established to cure *Mabs* infections and determining the  
387 susceptibility/resistance profile of clinical strains may greatly help the clinician to select

388 optimal drug treatments. It is worth mentioning that for this particular application, no  
389 absolute requirement for the tested strains to carry pTEC27 is needed, as visualization of  
390 fluorescent bacteria is not necessary if only assessing ZF survival. Second, since the ZF is  
391 particularly amenable to mimic a CF-like micro-environment, by silencing the *cftr* expression  
392 level (40), this system could be used to compare the therapeutic efficacy of clarithromycin  
393 and imipenem (and perhaps other antibiotics) in a *cftr*-deficient environment as it remains to  
394 be established whether a defect in CFTR affects susceptibility to drugs. Third, this method  
395 could be further exploited to compare the intrinsic activity of antibiotics *in vivo* in embryos  
396 infected with the three species of the *M. abscessus* complex - *M. abscessus sensu stricto*, *M.*  
397 *massiliense*, and *M. bolletii* - which are known to respond differently to antibiotics *in vitro*  
398 (41, 42).

399 Finally, the ZF embryo is particularly suited for high throughput screening as shown  
400 recently for *M. marinum* (36, 43, 44). Work is currently in progress in our laboratory to  
401 develop an *in vivo* platform for high-throughput screening of molecules against *Mabs* in order  
402 to speed up the process of identifying promising drug candidates, particularly warranted due  
403 to the extreme resistance of *Mabs* to most current antibiotics.

404

405 **ACKNOWLEDGMENTS**

406

407 We thank L. Ramakrishnan for the generous gift of pTEC27 and for helpful discussions. This  
408 study was supported by the french National Research Agency ([http://www.agence-](http://www.agence-nationale-recherche.fr/)  
409 [nationale-recherche.fr/](http://www.agence-nationale-recherche.fr/)) (ZebraFlam ANR-10-MIDI-009and DIMYVIR ANR-13-BSV3-0007-01),  
410 the European Community's Seventh Framework Programme (FP7-PEOPLE-2011-ITN) under  
411 grant agreement no. PITN-GA-2011-289209 for the Marie-Curie Initial Training Network  
412 FishForPharma. We wish also to thank Vaincre La Mucoviscidose  
413 (<http://www.vaincrelamuco.org/>) for funding A Bernut (RF2011 06000446) and V Le Moigne  
414 (RF20120600689) and the InfectioPôle Sud for funding part of the fish facility.

415

416

## 417 REFERENCES

- 418 1. **Medjahed H, Gaillard JL, Reytrat JM.** 2010. *Mycobacterium abscessus*: a new player in the  
419 mycobacterial field. Trends Microbiol. **18**:117-123.
- 420 2. **Petrini B.** 2006. *Mycobacterium abscessus*: an emerging rapid-growing potential pathogen.  
421 Apmis **114**:319-28.
- 422 3. **Roux AL, Catherinot E, Ripoll F, Soismier N, Macheras E, Ravilly S, Bellis G, Vibet MA, Le**  
423 **Roux E, Lemonnier L, Gutierrez C, Vincent V, Fauroux B, Rottman M, Guillemot D, Gaillard**  
424 **JL.** 2009. Multicenter study of prevalence of nontuberculous mycobacteria in patients with  
425 cystic fibrosis in France. J. Clin. Microbiol. **47**:4124-4128.
- 426 4. **Sanguinetti M, Ardito F, Fiscarelli E, La Sorda M, D'Argenio P, Ricciotti G, Fadda G.** 2001.  
427 Fatal pulmonary infection due to multidrug-resistant *Mycobacterium abscessus* in a patient  
428 with cystic fibrosis. J. Clin. Microbiol. **39**:816-819.
- 429 5. **Gilljam M, Schersten H, Silverborn M, Jonsson B, Ericsson Hollsing A.** 2010. Lung  
430 transplantation in patients with cystic fibrosis and *Mycobacterium abscessus* infection. J.  
431 Cyst. Fibros. **9**:272-276.
- 432 6. **Aitken ML, Limaye A, Pottinger P, Whimbey E, Goss CH, Tonelli MR, Cangelosi GA, Dirac**  
433 **MA, Olivier KN, Brown-Elliott BA, McNulty S, Wallace RJ, Jr.** 2012. Respiratory outbreak of  
434 *Mycobacterium abscessus* subspecies *massiliense* in a lung transplant and cystic fibrosis  
435 center. Am. J. Respir. Crit. Care Med. **185**:231-232.
- 436 7. **Wallace RJ, Jr, Brown BA, Griffith DE.** 1998. Nosocomial outbreaks/pseudo-outbreaks caused  
437 by nontuberculous mycobacteria. Annu. Rev. Microbiol. **52**:453-490.
- 438 8. **Viana-Niero C, Lima KV, Lopes ML, Rabello MC, Marsola LR, Brilhante VC, Durham AM,**  
439 **Leao SC.** 2008. Molecular characterization of *Mycobacterium massiliense* and *Mycobacterium*  
440 *bolletii* in isolates collected from outbreaks of infections after laparoscopic surgeries and  
441 cosmetic procedures. J. Clin. Microbiol. **46**:850-855.

- 442 9. **Zelazny AM, Root JM, Shea YR, Colombo RE, Shamputa IC, Stock F, Conlan S, McNulty S,**  
443 **Brown-Elliott BA, Wallace RJ, Jr, Olivier KN, Holland SM, Sampaio EP.** 2009. Cohort study of  
444 molecular identification and typing of *Mycobacterium abscessus*, *Mycobacterium*  
445 *massiliense*, and *Mycobacterium bolletii*. J. Clin. Microbiol. **47**:1985-1995.
- 446 10. **Cullen AR, Cannon CL, Mark EJ, Colin AA.** 2000. *Mycobacterium abscessus* infection in cystic  
447 fibrosis. Colonization or infection? Am. J. Respir. Crit. Care Med. **161**:641-645.
- 448 11. **Tomashefski JF, Jr., Stern RC, Demko CA, Doershuk CF.** 1996. Nontuberculous mycobacteria  
449 in cystic fibrosis. An autopsy study. Am. J. Respir. Crit. Care Med. **154**:523-528.
- 450 12. **Rodriguez G, Ortegon M, Camargo D, Orozco LC.** 1997. Iatrogenic *Mycobacterium abscessus*  
451 infection: histopathology of 71 patients. Br. J. Dermatol. **137**:214-218.
- 452 13. **Griffith DE, Aksamit T, Brown-Elliott BA, Catanzaro A, Daley C, Gordin F, Holland SM,**  
453 **Horsburgh R, Huitt G, Iademarco MF, Iseman M, Olivier K, Ruoss S, von Reyn CF, Wallace**  
454 **RJ, Jr., Winthrop K.** 2007. An official ATS/IDSA statement: diagnosis, treatment, and  
455 prevention of nontuberculous mycobacterial diseases. Am. J. Respir. Crit. Care Med. **175**:367-  
456 416.
- 457 14. **Jeon K, Kwon OJ, Lee NY, Kim BJ, Kook YH, Lee SH, Park YK, Kim CK, Koh WJ.** 2009.  
458 Antibiotic treatment of *Mycobacterium abscessus* lung disease: a retrospective analysis of 65  
459 patients. Am. J. Respir. Crit. Care Med. **180**:896-902.
- 460 15. **De Groote MA, Johnson L, Podell B, Brooks E, Basaraba R, Gonzalez-Juarrero M.** 2013. GM-  
461 CSF knockout mice for preclinical testing of agents with antimicrobial activity against  
462 *Mycobacterium abscessus*. J. Antimicrob. Chemother. **69**:1057-1064.
- 463 16. **Lerat I, Cambau E, Roth Dit Bettoni R, Gaillard JL, Jarlier V, Truffot C, Veziris N.** 2013. *In vivo*  
464 evaluation of antibiotic activity against *Mycobacterium abscessus*. J. Infect. Dis. **209**:905-912.
- 465 17. **Lavollay M, Dubee V, Heym B, Herrmann JL, Gaillard JL, Gutmann L, Arthur M, Mainardi JL.**  
466 2014. *In vitro* activity of ceftoxitin and imipenem against *Mycobacterium abscessus* complex.  
467 Clin. Microbiol. Infect. In Press.

- 468 18. **Cortes M, Singh AK, Reyrat JM, Gaillard JL, Nassif X, Herrmann JL.** 2011. Conditional gene  
469 expression in *Mycobacterium abscessus*. PLoS One **6**:e29306.
- 470 19. **Bernut A, Herrmann JL, Kissa K, Dubremetz JF, Gaillard JL, Lutfalla G, Kremer L.** 2014.  
471 *Mycobacterium abscessus* cording prevents phagocytosis and promotes abscess formation.  
472 Proc. Natl. Acad. Sci. USA **111**:E943-952.
- 473 20. **Talati NJ, Roupheal N, Kuppalli K, Franco-Paredes C.** 2008. Spectrum of CNS disease caused  
474 by rapidly growing mycobacteria. Lancet Infect. Dis. **8**:390-398.
- 475 21. **Lee MR, Cheng A, Lee YC, Yang CY, Lai CC, Huang YT, Ho CC, Wang HC, Yu CJ, Hsueh PR.**  
476 2011. CNS infections caused by *Mycobacterium abscessus* complex: clinical features and  
477 antimicrobial susceptibilities of isolates. J. Antimicrob. Chemother. **67**:222-225.
- 478 22. **Rottman M, Catherinot E, Hochedez P, Emile JF, Casanova JL, Gaillard JL, Soudais C.** 2007.  
479 Importance of T cells, gamma interferon, and tumor necrosis factor in immune control of the  
480 rapid grower *Mycobacterium abscessus* in C57BL/6 mice. Infect. Immun. **75**:5898-5907.
- 481 23. **Catherinot E, Clarissou J, Etienne G, Ripoll F, Emile JF, Daffe M, Perronne C, Soudais C,**  
482 **Gaillard JL, Rottman M.** 2007. Hypervirulence of a rough variant of the *Mycobacterium*  
483 *abscessus* type strain. Infect. Immun. **75**:1055-1058.
- 484 24. **Woods GL, Brown-Elliott BA, Conville PS, Desmond EP, Hall GS, Lin G, Pfyffer GE, Ridderhof**  
485 **JC, Siddiqi SH, Wallace RJ, Warren NG, Witebsky FG.** 2011. Susceptibility testing of  
486 mycobacteria, nocardiae, and other aerobic actinomycetes; approved standard, Second  
487 Edition. M24-A2. Clinical and Laboratory Standards Institute, Wayne, PA.
- 488 25. **Lamason RL, Mohideen MA, Mest JR, Wong AC, Norton HL, Aros MC, Jurynech MJ, Mao X,**  
489 **Humphreville VR, Humbert JE, Sinha S, Moore JL, Jagadeeswaran P, Zhao W, Ning G,**  
490 **Makalowska I, McKeigue PM, O'Donnell D, Kittles R, Parra EJ, Mangini NJ, Grunwald DJ,**  
491 **Shriver MD, Canfield VA, Cheng KC.** 2005. SLC24A5, a putative cation exchanger, affects  
492 pigmentation in zebrafish and humans. Science **310**:1782-1786.

- 493 26. **Adams KN, Takaki K, Connolly LE, Wiedenhoft, Winglee K, Humbert O, Edelstein PH, Cosma**  
494 **CL, Ramakrishnan L.** 2011. Drug tolerance in replicating mycobacteria mediated by a  
495 macrophage-induced efflux mechanism. *Cell* **145**:39-53.
- 496 27. **Lavollay M, Fourgeaud M, Herrmann JL, Dubost L, Marie A, Gutmann L, Arthur M, Mainardi**  
497 **JL.** 2011. The peptidoglycan of *Mycobacterium abscessus* is predominantly cross-linked by  
498 L,D-transpeptidases. *J. Bacteriol.* **193**:778-782.
- 499 28. **Medjahed H, Reytrat JM.** 2009. Construction of *Mycobacterium abscessus* defined  
500 glycopeptidolipid mutants: comparison of genetic tools. *Appl. Environ. Microbiol.* **75**:1331-  
501 1338.
- 502 29. **Howard ST, Rhoades E, Recht J, Pang X, Alsup A, Kolter R, Lyons CR, Byrd TF.** 2006.  
503 Spontaneous reversion of *Mycobacterium abscessus* from a smooth to a rough morphotype  
504 is associated with reduced expression of glycopeptidolipid and reacquisition of an invasive  
505 phenotype. *Microbiology* **152**:1581-1590.
- 506 30. **Zelmer A, Carroll P, Andreu N, Hagens K, Mahlo J, Redinger N, Robertson BD, Wiles S, Ward**  
507 **TH, Parish T, Ripoll J, Bancroft GJ, Schaible UE.** 2012. A new *in vivo* model to test anti-  
508 tuberculosis drugs using fluorescence imaging. *J. Antimicrob. Chemother.* **67**:1948-1960.
- 509 31. **Andreu N, Zelmer A, Sampson SL, Ikeh M, Bancroft GJ, Schaible UE, Wiles S, Robertson BD.**  
510 2013. Rapid *in vivo* assessment of drug efficacy against *Mycobacterium tuberculosis* using an  
511 improved firefly luciferase. *J. Antimicrob. Chemother.* **68**:2118-2127.
- 512 32. **Byrd TF, Lyons CR.** 1999. Preliminary characterization of a *Mycobacterium abscessus* mutant  
513 in human and murine models of infection. *Infect. Immun.* **67**:4700-4707.
- 514 33. **Oh CT, Moon C, Jeong MS, Kwon SH, Jang J.** 2013. *Drosophila melanogaster* model for  
515 *Mycobacterium abscessus* infection. *Microbes Infect.* **15**:788-795.
- 516 34. **Oh, C. T., C. Moon, O. K. Park, S. H. Kwon, and J. Jang.** 2014. Novel drug combination for  
517 *Mycobacterium abscessus* disease therapy identified in a *Drosophila* infection model. *J.*  
518 *Antimicrob. Chemother.* In Press.

- 519 35. **Squiban B, Kurz CL.** 2011. *C. elegans*: an all in one model for antimicrobial drug discovery.  
520 Curr. Drug Targets **12**:967-977.
- 521 36. **Takaki K, Cosma CL, Troll MA, Ramakrishnan L.** 2012. An *in vivo* platform for rapid high-  
522 throughput antitubercular drug discovery. Cell Rep. **2**:175-184.
- 523 37. **Takaki K, Davis JM, Winglee K, Ramakrishnan L.** 2013. Evaluation of the pathogenesis and  
524 treatment of *Mycobacterium marinum* infection in zebrafish. Nat. Protoc. **8**:1114-1124.
- 525 38. **Miyasaka T, Kunishima H, Komatsu M, Tamai K, Mitsutake K, Kanemitsu K, Ohisa Y,**  
526 **Yanagisawa H, Kaku M.** 2007. *In vitro* efficacy of imipenem in combination with six  
527 antimicrobial agents against *Mycobacterium abscessus*. Int. J. Antimicrob. Agents **30**:255-  
528 258.
- 529 39. **Shen GH, Wu BD, Hu ST, Lin CF, Wu KM, Chen JH.** 2010. High efficacy of clofazimine and its  
530 synergistic effect with amikacin against rapidly growing mycobacteria. Int. J. Antimicrob.  
531 Agents **35**:400-404.
- 532 40. **Phennicie RT, Sullivan MJ, Singer JT, Yoder JA, Kim CH.** 2010. Specific resistance to  
533 *Pseudomonas aeruginosa* infection in zebrafish is mediated by the cystic fibrosis  
534 transmembrane conductance regulator. Infect. Immun. **78**:4542-4550.
- 535 41. **Bastian S, Veziris N, Roux AL, Brossier F, Gaillard JL, Jarlier V, Cambau E.** 2011. Assessment  
536 of clarithromycin susceptibility in strains belonging to the *Mycobacterium abscessus* group by  
537 *erm(41)* and *rml* sequencing. Antimicrob. Agents Chemother. **55**:775-781.
- 538 42. **Kim HY, Kim BJ, Kook Y, Yun YJ, Shin JH, Kim BJ, Kook YH.** 2010. *Mycobacterium massiliense*  
539 is differentiated from *Mycobacterium abscessus* and *Mycobacterium bolletii* by erythromycin  
540 ribosome methyltransferase gene (*erm*) and clarithromycin susceptibility patterns. Microbiol.  
541 Immunol. **54**:347-353.
- 542 43. **Carvalho R, de Sonnevile J, Stockhammer OW, Savage ND, Veneman WJ, Ottenhoff TH,**  
543 **Dirks RP, Meijer AH, Spaink HP.** 2011. A high-throughput screen for tuberculosis  
544 progression. PLoS One **6**:e16779.

- 545 44. **Spaink HP, Cui C, Wiweger MI, Jansen HJ, Veneman WJ, Marin-Juez R, de Sonnevile J,**  
546 **Ordas A, Torraca V, van der Ent W, Leenders WP, Meijer AH, Snaar-Jagalska BE, Dirks RP.**  
547 2013. Robotic injection of zebrafish embryos for high-throughput screening in disease  
548 models. *Methods* **62**:246-254.  
549  
550

551 **FIGURE LEGENDS**

552

553 **Figure 1. Kinetics of colonization of *M. abscessus* in aerosolised or intravenously infected**554 **BALB/c mice. (A)** Mice were aerosolized by  $4 \times 10^7$  CFU/ml of R-*Mabs*. Animal were then

555 sacrificed at days 1, 3, 8, 27 prior to CFU counting in the liver, spleen and lungs. Results are

556 expressed as the log units of CFU. **(B)** Mice were challenged *i.v.*  $10^6$  CFU of R-*Mabs*. Animals

557 were then sacrificed at days 1, 15 and 30 to determine the CFU counts in the different

558 organs. Results are expressed as mean  $\text{Log}_{10}$  CFU from 2-3 independent experiments (n=5-7

559 mice for each time point). Error bars represent the standard error of the mean (SEM).

560

561 **Figure 2. Experimental protocol to assess the *in vivo* drug activity on *M. abscessus***562 **infection.** ZF embryos were *i.v.* infected with  $\approx 300$  CFU of R-*Mabs* expressing tdTomato and

563 distributed and incubated into 96-wells plate (1). From 1dpi, embryos were exposed to the

564 drugs of interest which were directly added to the wells. Drugs are then removed and daily

565 renewed for 5 days (2). To determinate the *in vivo* antibacterial effects of the drugs, the

566 embryo survival, the bacterial loads and the evolution of the infection process were

567 monitored at a spatiotemporal level by videomicroscopy (3).

568

569 **Figure 3. *In vivo* characterization of clarithromycin activity on *M. abscessus* infection. (A-F)**

570 Embryos were soaked in clarithromycin at 1.7X, 17X or 170X the MIC for 5 days. The red bar

571 indicates the start and duration of treatment. **(A)** Survival of uninfected embryos treated

572 with various doses of clarithromycin and compared to mock controls (DMSO 1%) (n=20 for

573 each, representative of three independent experiments). Representative microscopy image

574 of an untreated (inset, upper panel) or drug treated-embryo (inset, lower panel) at 8dpf.

575 Clarithromycin appears toxic at the highest concentration as evidenced by the development  
576 of abnormalities and the increased mortality rate in the drug-exposed embryos compared to  
577 the mock control ( $p=0.028$ , log-rank test). **(B)** Survival of infected *Mabs* treated at various  
578 doses of clarithromycin and compared to untreated infected embryos ( $\approx 300$  CFU,  $n=20$ ,  
579 representative of three independent experiments). A significant increased survival was  
580 observed in the infected-embryos exposed to the highest drug concentration ( $p=0.029$ , log-  
581 rank test). **(C)** Bacterial loads of untreated or treated-embryos ( $\approx 400$  CFU). Results are  
582 expressed as mean  $\text{Log}_{10}$  CFU per embryo from three independent experiments. A significant  
583 reduction in bacterial burdens with 170X the MIC in drug treated-embryos is observed at  
584 5dpi. **(D)** Spatiotemporal visualization of the infection by *Mabs* expressing dtTomato ( $\approx 300$   
585 CFU) in untreated or drug treated-embryos. The representative fluorescence and  
586 transmission overlay of whole embryos are shown. The yolk is auto-fluorescent. **(E)**  
587 Frequency of abscesses in whole untreated or drug treated-embryos over 13dpi ( $\approx 300$  CFU;  
588 average of three independent experiments). Infected embryos developed significantly less  
589 abscesses in the presence of clarithromycin at 170X the MIC than untreated infected-  
590 embryos. **(F)** Average localization of abscesses of the infected embryos in (E). *Mabs*-infected  
591 ZF developed significantly less abscesses within the brain and the spinal when exposed to  
592 the highest clarithromycin dose as compared to untreated infected-ZF. For (C) statistics were  
593 calculated using one-way ANOVA or for (E) and (F) with Fisher's exact test comparing each  
594 category of drug-treated embryos to untreated control. Error bars represent the SEM.  
595 \*\* $p<0.01$ .

596

597 **Figure 4. Imipenem treatment cures *M. abscessus*-infected embryos. (A-E)** From 1dpi,  
598 embryos were exposed for 5 days to imipenem concentrations corresponding to 0.5X, 5X or

599 28X the MIC. **(A)** Survival of infected R-*Mabs* embryos treated at various doses of imipenem  
600 and compared to untreated infected embryos ( $\approx 300$  CFU,  $n=20$ , representative of three  
601 independent experiments). Survival of treated R-*Mabs* infected embryos is dose-dependent.  
602 Significant increased survival was observed in infected-embryos exposed to 5 X and 28X MIC  
603 of imipenem. The red bar indicates the start and duration of treatment. **(B)** Bacterial loads of  
604 untreated or imipenem treated-embryos ( $\approx 400$  CFU). Results are expressed as mean  $\text{Log}_{10}$   
605 CFU per embryo from three independent experiments. A significant decreased of bacterial  
606 load is already observed after 3dpi in the 28X MIC imipenem treated-embryos. **(C)**  
607 Spatiotemporal visualization of the infection by R-*Mabs* expressing tdTomato ( $\approx 300$  CFU) in  
608 untreated or imipenem treated-embryos. The representative fluorescence and transmission  
609 overlay of whole embryos are shown. **(D)** Frequency of abscesses in whole untreated or  
610 imipenem-treated embryos over 13dpi ( $\approx 300$  CFU, average of three independent  
611 experiments). Only the 28X MIC imipenem treated-embryos developed significantly fewer  
612 abscesses than untreated infected-embryos. **(E)** Average localization of abscesses of the  
613 infected embryos in (D). 5X and 28X MIC of imipenem treated-embryos infected by *Mabs*  
614 developed fewer abscesses within the brain than untreated infected-embryos. For (B)  
615 statistics were calculated using one-way ANOVA or for (D) and (E) with Fisher's exact test  
616 comparing each category of imipenem-treated embryos to untreated control. Error bars  
617 represent the SEM. \* $p=0.02$ , \*\* $p<0.01$ , \*\*\* $p<0.001$ .

618

619 **Figure 5. Imipenem treatment decreases the early pathophysiological signs within the CNS.**

620 **(A-D).** tdTomato-expressing R-*Mabs* ( $\approx 300$  CFU) are injected in 30hpf embryos ( $n=15$ ,  
621 average of three independent experiments). From 1dpi, embryos were exposed to imipenem  
622 at 0.5X, 5X or 28X MIC during 5 days. **(A)** Fluorescence microscopy of a typical R serpentine

623 cord. Scale bar, 100 $\mu$ m. **(B)** Fluorescence and DIC overlay of whole heads of a 28X MIC  
624 imipenem-treated and untreated infected embryos with fluorescent R-Mabs showing  
625 serpentine cord (white arrow). Scale bars, 100 $\mu$ m. **(C)** Percentage of embryos with cords in  
626 whole untreated and imipenem-treated embryos at 4dpi. A significant reduction in the  
627 proportion of embryos with cords was observed when embryos were treated with the  
628 highest (28X MIC) imipenem concentration. **(D)** Average localization of cord within the  
629 infected embryos in (C). Infected embryos treated with the intermediate (5X MIC) and high  
630 (28X MIC) imipenem doses developed significantly fewer serpentine cords within the CNS  
631 compared to untreated infected-embryos. For (C) and (D), statistics were calculated using  
632 Fisher's exact test comparing each category of imipenem-treated embryos to untreated  
633 control. All results are expressed as the average from three independent experiments and  
634 error bars represent the SEM.  
635

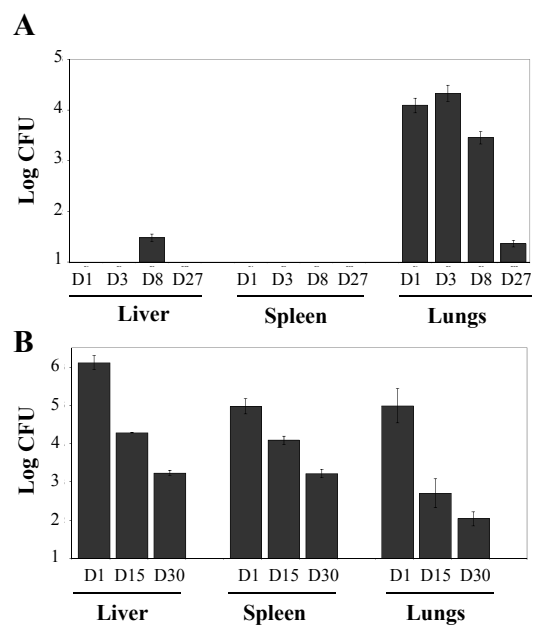


**Figure 1. Kinetics of colonization of *M. abscessus* in aerosolized or intravenously infected BALB/c mice. (A)** Mice were aerosolized by  $4 \times 10^7$  CFU/ml of *R-Mabs*. Animals were then sacrificed at days 1, 3, 8, 27 prior to CFU counting in the liver, spleen and lungs. Results are expressed as the log units of CFU. **(B)** Mice were challenged *i.v.*  $10^6$  CFU of *R-Mabs*. Animals were then sacrificed at days 1, 15 and 30 to determine the CFU counts in the different organs. Results are expressed as mean  $\text{Log}_{10}$  CFU from 2-3 independent experiments ( $n=5-7$  mice for each time point). Error bars represent the standard error of the mean (SEM).

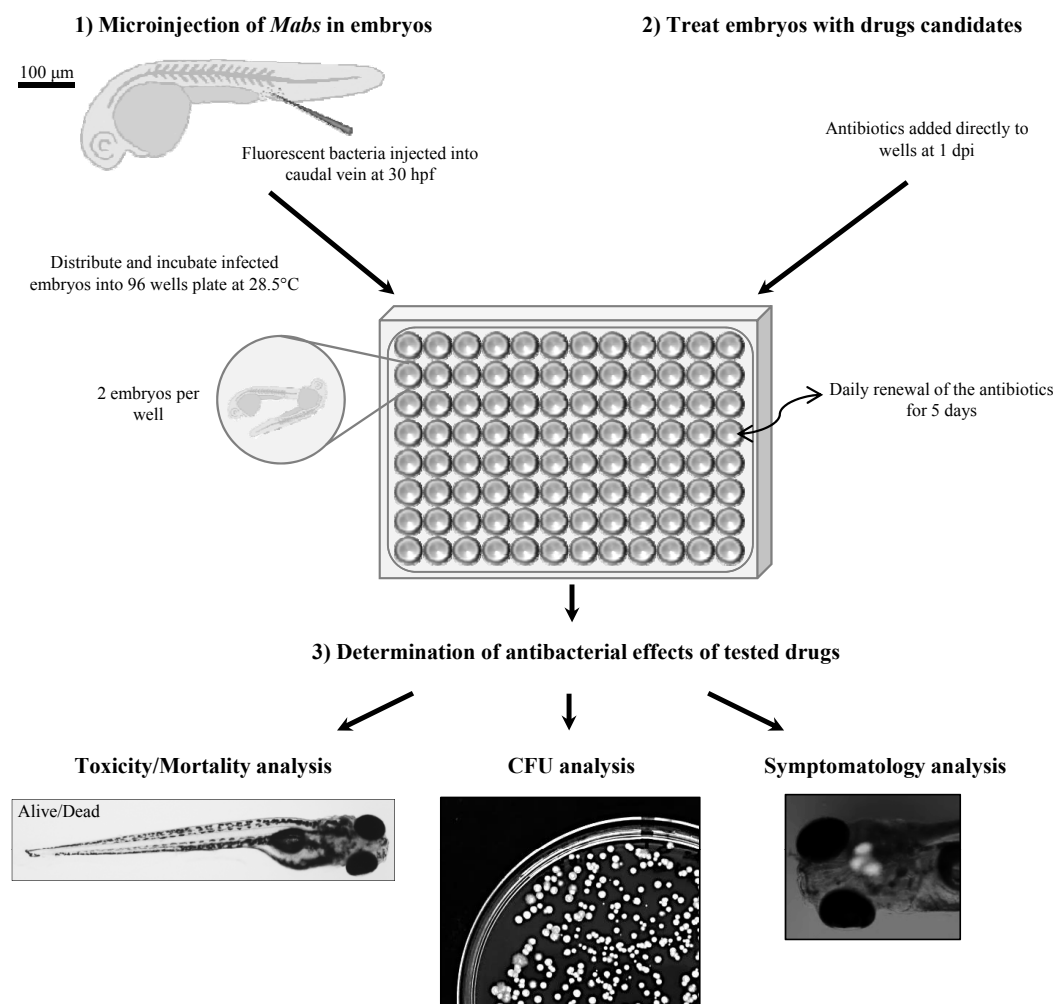


**Figure 2. Experimental protocol to assess the *in vivo* drug activity on *M. abscessus* infection.** ZF embryos were *i.v.* infected with  $\approx 300$  CFU of R-*Mabs* expressing tdTomato and distributed and incubated into 96-wells plate (1). From 1dpi, embryos were exposed to the drugs of interest which were directly added to the wells. Drugs are then removed and daily renewed for 5 days (2). To determinate the *in vivo* antibacterial effects of the drugs, the embryo survival, the bacterial loads and the evolution of the infection process were monitored at a spatiotemporal level by videomicroscopy (3).

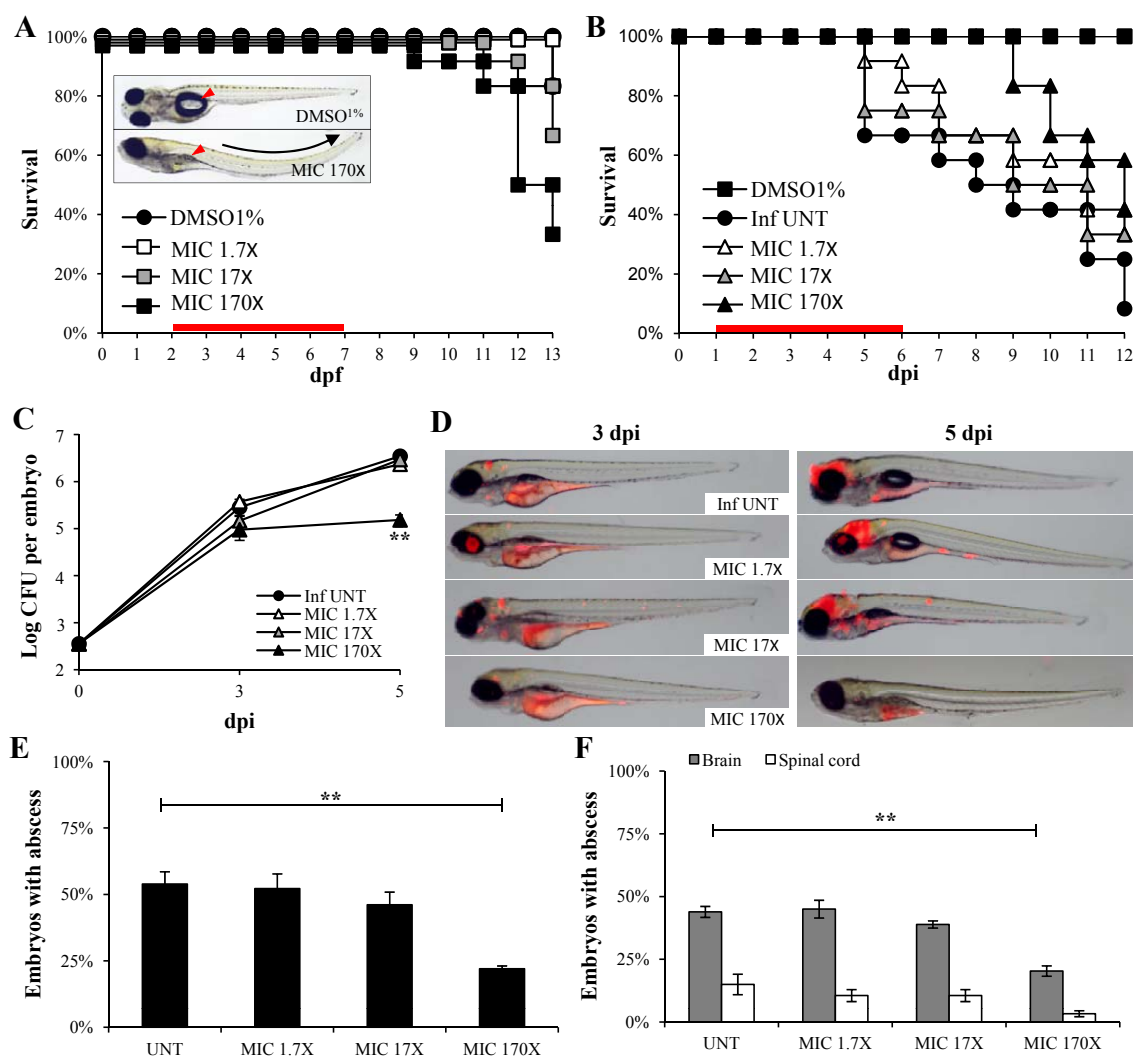


**Figure 3. In vivo characterization of clarithromycin activity on *M. abscessus* infection. (A-F)** Embryos were soaked in clarithromycin at 1.7X, 17X or 170X the MIC for 5 days. The red bar indicates the start and duration of treatment. **(A)** Survival of uninfected embryos treated with various doses of clarithromycin and compared to mock controls (DMSO 1%) ( $n=20$  for each, representative of three independent experiments). Representative microscopy image of an untreated (inset, upper panel) or drug treated-embryo (inset, lower panel) at 8dpf. Clarithromycin appears toxic at the highest concentration as evidenced by the development of abnormalities and the increased mortality rate in the drug-exposed embryos compared to the mock control ( $p=0.028$ , log-rank test). **(B)** Survival of infected *Mabs* treated at various doses of clarithromycin and compared to untreated infected embryos ( $\approx 300$  CFU,  $n=20$ , representative of three independent experiments). A significant increased survival was observed in the infected-embryos exposed to the highest drug concentration ( $p=0.029$ , log-rank test). **(C)** Bacterial loads of untreated or treated-embryos ( $\approx 400$  CFU). Results are expressed as mean  $\text{Log}_{10}$  CFU per embryo from three independent experiments. A significant reduction in bacterial burdens with 170X the MIC in drug treated-embryos is observed at 5dpi. **(D)** Spatiotemporal visualization of the infection by *Mabs* expressing dtTomato ( $\approx 300$  CFU) in untreated or drug treated-embryos. The representative fluorescence and transmission overlay of whole embryos are shown. The yolk is auto-fluorescent. **(E)** Frequency of abscesses in whole untreated or drug treated-embryos over 13dpi ( $\approx 300$  CFU; average of three independent experiments). Infected embryos developed significantly less abscesses in the presence of clarithromycin at 170X the MIC than untreated infected-embryos. **(F)** Average localization of abscesses of the infected embryos in (E). *Mabs*-infected ZF developed significantly less abscesses within the brain and the spinal when exposed to the highest clarithromycin dose as compared to untreated infected-ZF. For (C) statistics were calculated using one-way ANOVA or for (E) and (F) with Fisher's exact test comparing each category of drug-treated embryos to untreated control. Error bars represent the SEM. **\*\*** $p<0.01$ .

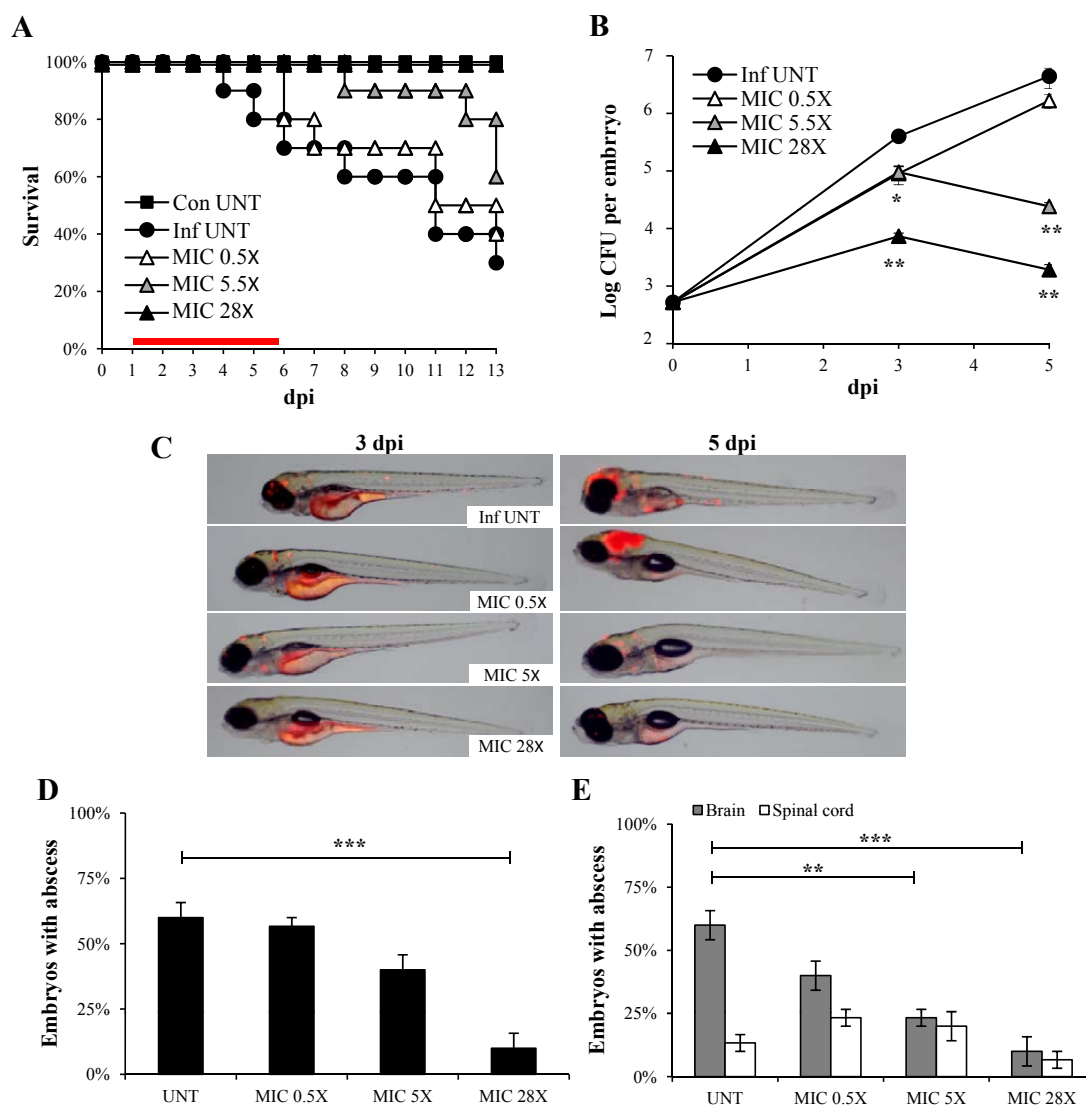


**Figure 4. Imipenem treatment cures *M. abscessus*-infected embryos. (A-E)** From 1dpi, embryos were exposed for 5 days to imipenem concentrations corresponding to 0.5X, 5X or 28X the MIC. **(A)** Survival of infected R-*Mabs* embryos treated at various doses of imipenem and compared to untreated infected embryos ( $\approx 300$  CFU,  $n=20$ , representative of three independent experiments). Survival of treated R-*Mabs* infected embryos is dose-dependent. Significant increased survival was observed in infected-embryos exposed to 5 X and 28X MIC of imipenem. The red bar indicates the start and duration of treatment. **(B)** Bacterial loads of untreated or imipenem treated-embryos ( $\approx 400$  CFU). Results are expressed as mean  $\text{Log}_{10}$  CFU per embryo from three independent experiments. A significant decreased of bacterial load is already observed after 3dpi in the 28X MIC imipenem treated-embryos. **(C)** Spatiotemporal visualization of the infection by R-*Mabs* expressing tdTomato ( $\approx 300$  CFU) in untreated or imipenem treated-embryos. The representative fluorescence and transmission overlay of whole embryos are shown. **(D)** Frequency of abscesses in whole untreated or imipenem-treated embryos over 13dpi ( $\approx 300$  CFU, average of three independent experiments). Only the 28X MIC imipenem treated-embryos developed significantly fewer abscesses than untreated infected-embryos. **(E)** Average localization of abscesses of the infected embryos in (D). 5X and 28X MIC of imipenem treated-embryos infected by *Mabs* developed fewer abscesses within the brain than untreated infected-embryos. For (B) statistics were calculated using one-way ANOVA or for (D) and (E) with Fisher's exact test comparing each category of imipenem-treated embryos to untreated control. Error bars represent the SEM. \* $p=0.02$ , \*\* $p<0.01$ , \*\*\* $p<0.001$ .

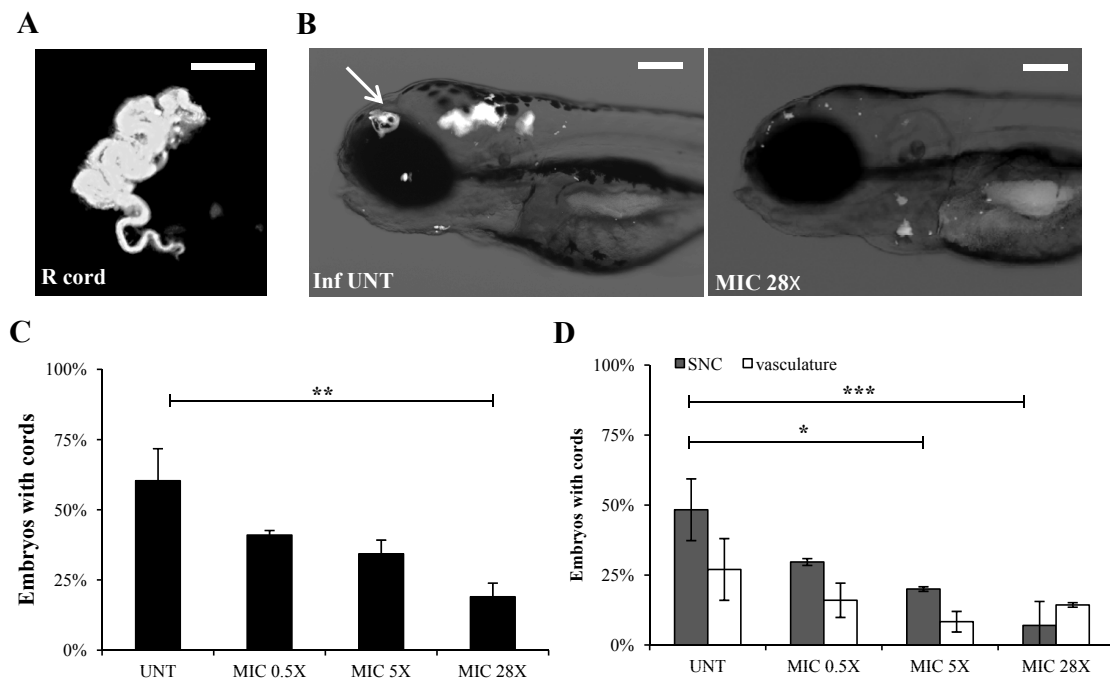


**Figure 5. Imipenem treatment decreases the early pathophysiological signs within the CNS. (A-D).** tdTomato-expressing *R-Mabs* ( $\approx 300$  CFU) are injected in 30hpf embryos ( $n=15$ , average of three independent experiments). From 1dpi, embryos were exposed to imipenem at 0.5X, 5X or 28X MIC during 5 days. **(A)** Fluorescence microscopy of a typical R serpentine cord. Scale bar,  $100\mu\text{m}$ . **(B)** Fluorescence and DIC overlay of whole heads of a 28X MIC imipenem-treated and untreated infected embryos with fluorescent *R-Mabs* showing serpentine cord (white arrow). Scale bars,  $100\mu\text{m}$ . **(C)** Percentage of embryos with cords in whole untreated and imipenem-treated embryos at 4dpi. A significant reduction in the proportion of embryos with cords was observed when embryos were treated with the highest (28X MIC) imipenem concentration. **(D)** Average localization of cord within the infected embryos in (C). Infected embryos treated with the intermediate (5X MIC) and high (28X MIC) imipenem doses developed significantly fewer serpentine cords within the CNS compared to untreated infected-embryos. For (C) and (D), statistics were calculated using Fisher's exact test comparing each category of imipenem-treated embryos to untreated control. All results are expressed as the average from three independent experiments and error bars represent the SEM.